Virtual long term testing of high-power fiber lasers

J. Schüttler, B. Neumann, S. Belke, F. Becker, and S. Ruppik
Coherent | ROFIN, Berzeliusstrasse 87, D-22113 Hamburg, Germany

Introduction

The remarkable power scaling of high power fiber lasers over the past years has become more and more challenging, because the effects of transverse mode instability (TMI) and photodarkening (PD) of the fiber are limiting the effective output power of typical industrial fiber lasers.

The origin of the TMI is a power transfer from the fundamental mode of the fiber to higher transverse modes via self-induced long-period gratings in the fiber due to the thermo-optical effect [1]. The excitation of higher modes can lead to temporal instability of the laser power, and to an increased power transfer from the core to the cladding via bend losses, thus reducing the effective laser power. Over the lifetime of a fiber laser, the TMI threshold is decreasing due to photodarkening of the active fiber core [2]. This can lead to a degradation of the laser performance over several thousand hours of operation.

Regarding a short time-to-market, the time-consuming lifetime testing of early prototypes is a major drawback in the development of new products. The goal of this work is to develop a reliable way to predict the performance of a certain laser setup including fiber design, pump and resonator configuration, and fiber routing prior to the actual prototype build. Testing of the final design is not replaced by the simulation, but it enables to compare variants in order to avoid unnecessary design iterations.

Many investigations have been made to understand, model and simulate both TMI and PD, but the microscopic mechanisms are not yet fully understood [3–6]. The existing models are usually either comprehensive, but very slow and therefore limited to the simulation of rather short fibers, or reduced models that do not take transverse effects into account. In [7] an approach has been demonstrated to simulate TMI in a fiber amplifier including the influence of back-reflections, thus incorporating forward and backward propagating light in the model. However, the model makes use of an idealized step-index fiber having eigenmodes that can be analytically described. Transverse inhomogeneities (such as realistic index or doping profiles) as well as photodarkening-induced lowering of the TMI threshold are not captured by this model.

Outline of the Modelling Approach

It is widely agreed that the dominant contribution to TMI in high-power fiber lasers are thermo-optical long-period index gratings in the fiber due to the transversely inhomogeneous heat load (and thus temperature profile) in the fiber. This heat load is mainly caused by the quantum defect and an additional heating of the fiber due to photodarkening-induced absorption. Both contributions depend on the transverse distribution of inversion, which is non-homogeneous even in an idealized step-index fiber and even more complicated for real fibers with non-idealized index and doping profiles.

A full 3D model capturing the longitudinal variations along the fiber as well as the transverse effects with a sufficient resolution would result in a huge number of numerical degrees of freedom. Because of limitations in computational resources and time, this approach is obviously not feasible. Furthermore, mode coupling dynamics and photodarkening have completely different time scales, so a coupled simulation of both effects is not desirable for the same reason.

In this work we present a numerical approach where the different time and length scales are separated, resulting in a highly efficient numerical scheme where the long-term degradation of the fiber properties due to photodarkening and its impact on the TMI threshold are considered, including the radially varying time scales of the degradation. The basic idea of this approach is to separate the time and length scales of the problem as follows: Assuming that the properties of the fiber are constant over its length, and the relevant quantities influencing PD and TMI are only dependent on the mode powers and their longitudinal variation, it is sufficient to consider the transverse two-dimensional (2D) cross section of the fiber to calculate effective average absorption or mode coupling coefficients first, and then solve a set of one-dimensional (1D) mode amplitude equations for the longitudinal distribution of mode powers. As the photodarkening takes place on a much

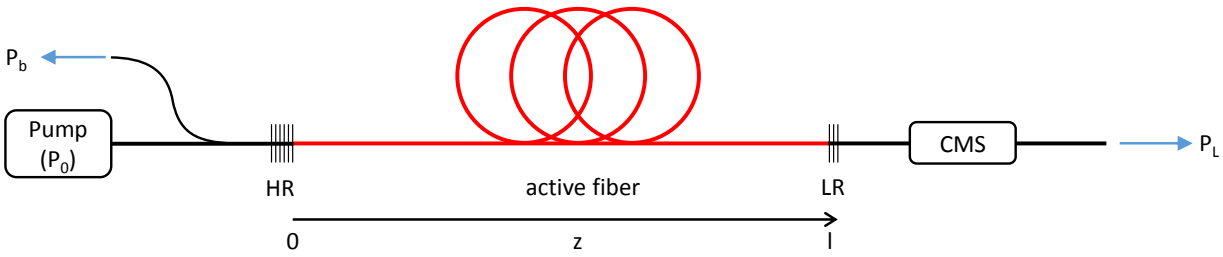

Figure 1: Schematic layout of the experimental setup consisting of active (red) and passive (black) LMA fibers, high reflective (HR) and low reflective (LR) FBGs, a pump module providing a pump power P_0 and a cladding mode stripper (CMS). l denotes the active fiber length along the z-direction, P_L is the laser output power (LP_{01} only) and P_b the sum of backwards propagating core and cladding power transmitted by the HR FBG.

longer timescale than any laser dynamics, the 2D and 1D problems are treated as stationary solutions, which are solved parametrically over the desired virtual testing time.

In the following section, first the experimental setup used for calibration and validation of the model is described. Afterwards, the numerical model is presented, and the results are discussed.

Experimental Setup

The numerical approach is validated using an experimental setup which is designed to exaggerate the effects of TMI and PD by means of a fiber and oscillator configuration resulting in relatively high heat loads and inversion levels compared to standard fibers or laser products. The setup is basically an all-in-fiber laser oscillator in co-pumped configuration, as shown in Figure 1, producing > 1 kW of output power. The oscillator is formed by low reflective (LR) and high reflective (HR) fiber Bragg gratings (FBGs) inscribed into a passive large mode area (LMA) fiber matching the active fiber, an ytterbium (Yb) doped LMA fiber. The used active and passive fibers have a 20 µm core and 400 µm cladding diameter.

The fiber is routed on a water-cooled base plate in a way that higher order modes are effectively transferred from the core to the cladding due to bend losses. The pump power is provided by fiber-coupled diode laser modules at 976 nm and launched at the HR end of the laser oscillator. On the output side, cladding mode strippers (CMS) ensure that the core light can be measured independently of the cladding light. Additionally, at the HR side the backward propagating core and cladding light can be monitored as well.

Numerical Modeling

a) Photodarkening

The temporal evolution of the photodarkening losses is calculated by the commonly accepted stretched exponential function

$$\alpha_{PD}(t) = \alpha_{sat}\left(1 - \exp\left(-(t/\tau)^{\beta}\right)\right) \tag{1}$$

with the stretching exponent β, the local timescale

$$\frac{1}{\tau} = \frac{1}{\tau_0}\left(\frac{N_2}{N}\right)^{C} \tag{2}$$

and the saturated PD absorption (according to Ref. [8])

$$\alpha_{sat} = \frac{A}{\mu}\left(\frac{N}{N_{ref}}\right)^{S}\frac{N_2/N}{0.46}, \tag{3}$$

where N is the local doping concentration, $N_{ref} = 8.74 \cdot 10^{25}\,\mathrm{m}^{-3}$ is a reference concentration, N_2 is the number of excited Yb ions, $\mu \approx 71$ (Ref. [9]) is a factor relating the absorption at the laser wavelength (1070 nm) to the absorption in the measurement setup at 633 nm. The values for A, C, S, β and τ_0 are determined from accelerated photodarkening experiments.

It is worth noting that neither the photodarkening level after a given time interval nor the photodarkening rate is constant over a transverse cross section of the fiber core, but both depend on the local inversion level, which is typically higher at the core edge than in the center due to the mode shape and the resulting gain saturation. Therefore, the equations (1)-(3) are treated as local, i. e. they apply to any point $\{r, \varphi, z\}$ in the transverse (r, φ) and longitudinal (z) dimensions of the fiber.

b) Transverse Model

In order to calculate the local PD rates and the resulting PD absorption after a given time of laser operation at nominal power, the transverse distribution of the inversion has to be calculated. This is achieved by first calculating the mode shapes for a given fiber design using the *Electromagnetic Waves, Frequency Domain* interface in COMSOL® Multiphysics. The 2D eigenmode problem is solved for a radial index profile $n(r)$, where n is the refractive index and r the radial coordinate of the fiber cross section.

The normalized electric field distributions ("mode shapes") of the LP_{01} and LP_{11} mode are $\psi_{01}(r)$ and $\psi_{01}(r,\varphi)$, respectively, with $\langle\psi_{01}^2\rangle = 1$ and $\langle\psi_{11}^2\rangle = 1$. The transverse integration operator $\langle\ldots\rangle$ is implemented in COMSOL® using domain probes that integrate over the cross section of the fiber.

For the calculation of the inversion profile and the resulting gain/absorption coefficients, an incoherent addition of the mode powers is assumed, which agrees very well with the longitudinal average over at least the intermodal beat length (IMBL) in a coherent calculation. In this case, for any given combination of pump power P_p and mode powers P_{01} and P_{11}, the local light intensities for pump and signal light are $I_p = P_p/(\pi r_0^2)$ and

$$I_s = I_{si}(r,\varphi) = \frac{P_{01}^{tot}\psi_{01}^2(r) + P_{11}^{tot}\psi_{11}^2(r,\varphi)}{\pi r_0^2}. \quad (4)$$

Here, the total powers of the LP_{01} and LP_{11} modes are $P_{01}^{tot} = P_{01}^{+} + P_{01}^{-}$ and $P_{11}^{tot} = P_{11}^{+} + P_{11}^{-}$, and r_0 is the cladding radius of the fiber. The local stationary inversion is calculated according to

$$\frac{N_2(r,\varphi)}{N(r)} = \frac{I_p\nu_s\sigma_{ap} + I_s\nu_p\sigma_{as}}{I_p\nu_s(\sigma_{ap}+\sigma_{ep}) + I_s\nu_p(\sigma_{as}+\sigma_{es}) + h\gamma_{se}\nu_s\nu_p} \quad (5)$$

with the optical frequencies $\nu_{p,s}$ for pump (index p) and signal (s) light, and the effective cross sections $\sigma_{a,e/p,s}$ for absorption (a) and emission (e). h is Planck's constant and γ_{se} is the rate of spontaneous emission from the upper lasing state.

The local signal and pump absorption at any point in the fiber cross section is calculated as

$$\alpha_{p,s} = -(\sigma_{ep,s} + \sigma_{ap,s})N_2(r,\varphi) + \sigma_{ap,s}N(r). \quad (6)$$

Assuming that the mode shapes are not affected by gain or losses, effective absorption coefficients for the mode powers are obtained:

$$\alpha_p^{eff} = \langle\alpha_p(r,\varphi)\rangle \quad (7)$$

and

$$\alpha_{01,11}^{eff} = \left\langle\psi_{01,11}^2(r,\varphi)\left(\alpha_s(r,\varphi) + \alpha_{PD}(r,\varphi)\right)\right\rangle. \quad (8)$$

For the calculation of the mode coupling by the asymmetric temperature profile, a coherent addition is used with a relative phase of 0 between LP_{01} and LP_{11}:

$$I_s = I_{sc}(r,\varphi) = \frac{\left(A_{01}\psi_{01}(r) + A_{11}\psi_{11}(r,\varphi)\right)^2}{\pi r_0^2}. \quad (9)$$

Here, A_{01} and A_{11} are the scalar field amplitudes, with $P_{01} = |A_{01}|^2$ and $P_{11} = |A_{11}|^2$. $P_{ij} = |A_{ij}|^2$

The local (volumetric) heat load follows from the energy balance of the quantum defect (note that negative values of α_s imply gain):

$$q_{QD} = I_p\alpha_p(r,\varphi) + I_{sc}(r,\varphi)\alpha_s(r,\varphi), \quad (10)$$

and the heat load from the signal absorption due to photodarkening is

$$q_{PD}(t) = I_{sc}(r,\varphi)\alpha_{PD}(t,r,\varphi). \quad (11)$$

For each combination of P_p, P_{01} and P_{11}, the stationary heat equation

$$-k\nabla_\perp^2 T = q_{QD} + q_{PD} \quad (12)$$

is solved using the *Heat Transfer in Solids* interface with $T(r_0) = T_0$ at the outer perimeter of the cladding, and $\delta T = T - T_0$ is defined. The amplitude of the thermo-optical grating, and hence the coupling efficiency is then calculated as

$$\hat{\alpha}_{MC} = n_0 k_s \frac{\partial n}{\partial T}\langle\delta T\psi_{01}(r)\psi_{11}(r,\varphi)\rangle \quad (13)$$

with the vacuum wavenumber $k_0 = 2\pi\nu_s/c$ of the signal light and the average refractive index n_0 of the fiber.

In a fully coherent approach – e. g. as in Ref. [7] – the effect of the asymmetric index profile (Eq. (13)) is modulated in space and time by the wavenumber and frequency difference of the competing modes, leading to a (generally moving) long period grating, which transfers energy back and forth between the modes on short scales. The effective amplitude of the grating is reduced by longitudinal heat diffusion and incoherent addition of several longitudinal modes travelling in both directions. This can lead to a much lower average energy transfer rates on larger spatiotemporal scales.

It turns out that for a large parameter range this longitudinally averaged mode coupling rate is very well approximated by scaling the calculated, fully coherent mode coupling coefficient $\hat{\alpha}_{MC}$ by a dimensionless parameter $c_{MC} \approx 1/20 \ldots 1/10$, which gives rise to a simplified modeling of the effective mode coupling strength as discussed below.

c) Longitudinal Model

The dependencies of gain, absorption and mode coupling rates from the local pump and signal powers are exported using probe tables that are used to build interpolation functions in the longtitudinal model. In the latter, the fiber laser is modelled as a one-dimensional device of length l (corresponding to the length of the active fiber in the real laser), neglecting the transverse dimensions of the fiber. The light is propagating along the positive or negative z direction, respectively, where the HR FBG is located at $z = 0$ and the LR FBG is located at $z = l$. In COMSOL® Multiphysics a number of *Coefficient Form PDE* interfaces is used for the 1D model.

The propagation of light in different modes in the fiber is described by the following equations for pump light ($P_p^+(z) = P_p(z)$), forward (+) and backward (–) propagating light in the LP_{01} ($P_{01}^{\pm}(z) = |A_{01}^{\pm}(z)|^2$) and LP_{11} ($P_{11}^{\pm}(z) = |A_{11}^{\pm}(z)|^2$) mode respectively, and forward and backward propagating light at signal wavelength in the fiber cladding ($P_c^{\pm}(z)$). The equations for the LP_{01} and LP_{11} modes are formulated as field amplitudes rather than powers to maintain the energy conservation of the mode coupling properly.

$$\partial_z P_p = -\alpha_p^{eff} P_p \,, \tag{14}$$

$$\pm\partial_z A_{01}^{\pm} = -\tfrac{1}{2}\alpha_{01}^{eff} A_{01}^{\pm} - \gamma_{MC}^{eff} A_{11}^{\pm} \,, \tag{15}$$

$$\pm\partial_z A_{11}^{\pm} = -\tfrac{1}{2}\alpha_{11}^{eff} A_{11}^{\pm} + \gamma_{MC}^{eff} A_{01}^{\pm} - \tfrac{1}{2}\alpha_{BL} A_{11}^{\pm} \,, \tag{16}$$

and

$$\pm\partial_z P_c^{\pm} = \alpha_{BL} P_{11}^{\pm} \,, \tag{17}$$

where α_{01}^{eff}, α_{11}^{eff} and α_p^{eff} are the effective absorption (or gain, if negative) coefficients for LP_{01}, LP_{11} and pump light, respectively. These coefficients all depend on P_p, $P_{01}^{tot} = P_{01}^+ + P_{01}^-$, $P_{11}^{tot} = P_{11}^+ + P_{11}^-$ and are precalculated as interpolation functions using Eqs. (4)-(7). The coefficient $\alpha_{BL}(z)$ describes the longitudinal distribution of the bend losses (according to the fiber routing) which transfer power from the LP_{11} mode to the cladding (Eq. (17)).

The effective mode coupling between LP_{01} and LP_{11} is modeled by the coefficient $\gamma_{MC}^{eff} = c_{MC}\hat{\alpha}_{MC}$, which is derived from the self-consistent thermo-optical index profile of the coherent addition of both modes (Eqs. (9) and (13)).

The boundary conditions are: $P_p(z=0) = P_0$, $P_c^+(0) = 0$, $P_c^-(l) = 0$ and the following equations apply at the FBGs:

$$P_{01}^+(0) = \rho_{HR}(1-\kappa)P_{01}^-(0) + \kappa P_{11}^-(0) \tag{18}$$

$$P_{11}^+(0) = \rho_{HR}(1-\kappa)P_{11}^-(0) + \kappa P_{01}^-(0) \tag{19}$$

$$P_{01}^-(l) = \rho_{LR}(1-\kappa)P_{01}^+(l) + \kappa P_{11}^+(l) \tag{20}$$

$$P_{11}^-(l) = \rho_{LR}(1-\kappa)P_{11}^+(l) + \kappa P_{01}^+(l) \tag{21}$$

with the (power) reflectivities $\rho_{HR,LR}$ at the HR and LR FBG respectively, and a mode mixing coefficient $\kappa \ll 1$ that accounts for a small amount of intermodal energy transfer due to splice imperfections.

In this work, the amplitude equations for the modal content are an incoherent approximation neglecting short-scale effects like mode beating, interference etc. The mode coupling is modeled as an effective transfer rate, which scales linearly with the precalculated mode coupling strength (Eq. (13)) due to the thermo-optical effect and is calibrated against the experimental results once. A major advantage of the incoherent formulation is the numerical efficiency, as the IMBL does not need to be resolved by the numerical grid. This way, extended parameter studies can be performed on a time scale of hours instead of days or weeks.

Simulation Results

The simulation of the long-term behavior of the laser setup is divided into two steps. First, for a given fiber design the 2D eigenvalue problem is solved to obtain the mode shapes ψ_{01} and ψ_{11} and the bend losses depending on the fiber bend radius. In a second step, Eqs. (4)-(13) are solved for a reasonable range of parameter combinations of P_p, P_{01}^{tot} and P_{11}^{tot}, and for the desired evaluation times t, which correspond to the virtual long-term testing time, typically in the range of several 1000 h. The evaluated effective absorptions, heat loads and coupling terms are used to build multidimensional interpolation functions, e. g. $\alpha_{01}^{eff} = \alpha_{01}^{eff}(P_p, P_{01}^{tot}, P_{11}^{tot})$ or $\gamma_{MC}^{eff} = \gamma_{MC}^{eff}(P_p, P_{01}^{tot}, P_{11}^{tot}, t)$. This precalculation of the interpolation functions is the most time consuming part and requires typically less than 1 h up to several hours depending on the required range and resolution of the interpolated data.

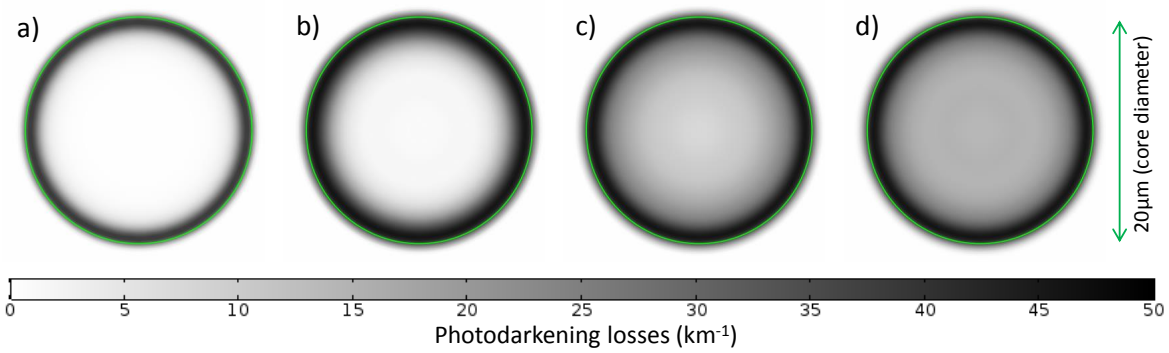

Figure 2: Simulated spatial distribution of photodarkening losses in a fiber cross section after a) $t = 10\,\text{h}$, b) $t = 100\,\text{h}$, c) $t = 1\,000\,\text{h}$, d) $t = 10\,000\,\text{h}$. Green lines indicate the border of the fiber core.

In the second step, Eqs. (14)-(21) are solved in the following sequence of parametric sweeps, using the previously determined interpolation functions: First, for $t = 0$ the input pump power P_0 is varied to obtain the performance characteristic $P_L(P_0)$ ("power curve") of the virtual laser. The output power of the virtual laser is defined as $P_L = (1-\rho_{LR})P_{01}^{+}(z=l)$.

Next, the pump power that corresponds to the nominal output power of the laser is determined – i. e. the power, at which the real laser would run in a physical long-term test. This pump power value is then kept constant, and the values for $\alpha_{PD}(z,t) = \alpha_{PD}(P_p(z), P_{01}^{tot}(z), P_{11}^{tot}(z), t)$ are calculated with the self-consistent solutions $P_p(z)$, $P_{01}^{tot}(z)$ and $P_{11}^{tot}(z)$ for each t. Finally, power ramps for each t are calculated, using the previously calculated values of $\alpha_{PD}(z,t)$.

The complete simulation sequence covering a virtual test duration of typically 100 000 h usually takes only a few hours on an 8–16 core workstation, which is orders of magnitude faster than any attempt to solve the fully coupled 3D system, taking the number of parameter variations into account.

In the following, some typical results of the presented numerical approach are presented. Figure 2 exemplifies the virtual aging of the fiber at evaluation times $t = 10\,\text{h}$, $t = 100\,\text{h}$, $t = 1\,000\,\text{h}$ and $t = 10\,000\,\text{h}$ for parameters P_p, P_{01} and P_{11} that correspond to typical values at the HR end of the fiber, where the pump power, heat load and inversion are higher than anywhere else in the modeled co-pumped laser resonator. The photodarkening becomes visible at the outer edge of the fiber core first, where the low intensity in the tail of the LP_{01} mode is not able to fully saturate the gain, and therefore the inversion is higher than in the center. This results in a short timescale for photodarkening according to Eq. (2) at the outer core perimeter. As a consequence, the photodarkening losses are almost saturated in this example after only 100 h, while in the center the photodarkening has not even become visible due to the low inversion.

After 10 000 h, the photodarkening losses are stabilizing while approaching the saturated value α_{sat} in most parts of the fiber cross section. Here, it becomes obvious that also α_{sat} strongly depends on the inversion: it is highest in regions with relatively high inversion at the core perimeter. On the other hand, higher PD losses in the outer region of the core have only a minor contribution to the total losses, because the intensity of the fundamental mode is low there as well (cf. Eq. (7)).

In the following, results of the longitudinal model are compared to experimental results for different laser setups, using the precalculated data from the transverse model. The simulated output power P_L is directly comparable to the output power measured behind the CMS in the experiment. The backward power, defined as $P_b = (1-\rho_{HR})(P_{01}^{-}(0) + P_{11}^{-}(0)) + P_c^{-}(0)$, is compared to the back power signal in the experiment, which monitors the sum of the remaining core light transmitted by the HR FBG and the backward cladding light. A nonlinear increase in the backward power is an indication for TMI, because the LP_{11} power is increased and then quickly transferred to the cladding. As the only source for cladding power in the presented model are the bend losses for the LP_{11} mode (Eq. (17)), P_c is proportional to the total amount of higher order mode power created in the fiber.

Figure 3 clearly demonstrates the PD induced lowering of the TMI threshold in the simulation as well as in the experiment. The scaling coefficient c_{MC} was calibrated to reproduce the experimental power curve

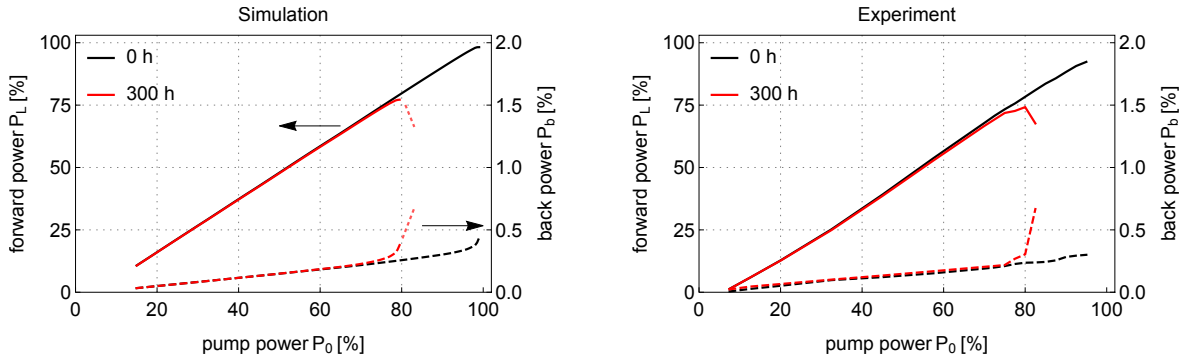

Figure 3: Simulated (left) and experimental (right) power curves for a laser setup with high inversion and heat load. Solid / left axis: forward power (LP_{01}), dashed / right axis: back power (core and cladding). Black: $t = 0\,\mathrm{h}$, red: $t = 300\,\mathrm{h}$. Dotted lines are visual guidelines only, see text for details.

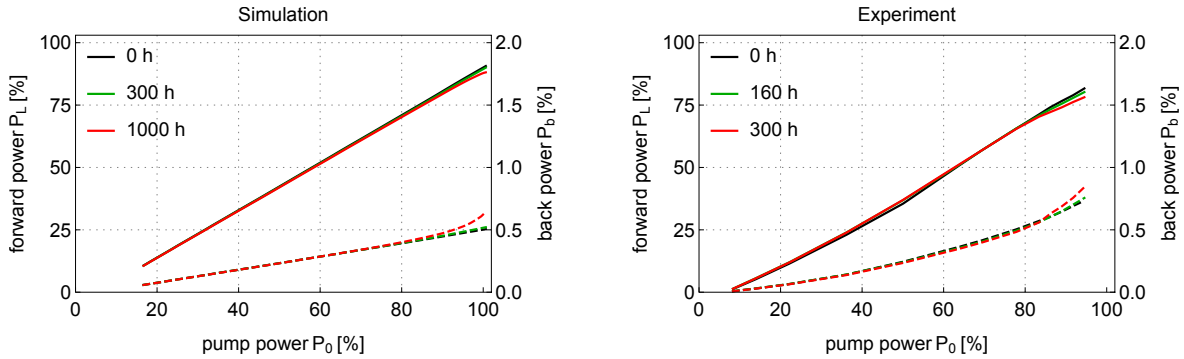

Figure 4: Simulated (left) and experimental (right) power curves for a laser setup with lower inversion. Solid / left axis: forward power (LP_{01}), dashed / right axis: back power (core and cladding). Black: $t = 0\,\mathrm{h}$, green: $t = 300\,\mathrm{h}$ (simulation) / $t = 160\,\mathrm{h}$ (experiment) red: $t = 1000\,\mathrm{h}$ (simulation) / $t = 300\,\mathrm{h}$ (experiment).

at $t = 0\,\mathrm{h}$, and was then kept constant for all following simulations.

For $t = 0\,\mathrm{h}$, a small increase of the back power is observed in the experiment for $P_0 > 90\%$, and the power curve is starting to roll over very slightly at the maximum power accordingly. After 300 h, the threshold for TMI is lowered significantly to about 80% pump power due to photodarkening. Because of the dynamic nature of TMI, it is not possible to find a stationary solution numerically above the threshold. Therefore, the dotted lines in Fig. 3 are only guidelines for a better visualization. The presented model is not capable of simulating the effects of fully developed TMI. However, it can predict the TMI *threshold* with high accuracy, which was the main goal of this work, and which is demonstrated in Fig. 3.

Figure 4 shows power curves for a different laser setup, where the resonator parameters have been changed to reduce the average inversion level in the active fiber. Again, for $t = 0\,\mathrm{h}$ no TMI is observed up to the maximum laser power. In contrast to the first setup, where after 300 h the TMI threshold was significantly lowered, in this setup only a slight degradation is visible above $\approx 75\%$ pump power, and the back power is starting to increase. The numerical results reproduce this behaviour, even if the time scales are slightly longer in the simulation. It should be noted that the temporal evolution of the PD absorption (Eq. 1) is very steep in the beginning and flattens for larger values of t. Consequently, small uncertainties in the fitting parameters have the greatest impact at the beginning of the PD process.

However, the tendency of lowering the PD impact and slowing down the PD induced aging by lower inversion levels is clearly demonstrated in the experiment as well as in the simulation.

The previously discussed setups were designed for demonstrating the effects under investigation using

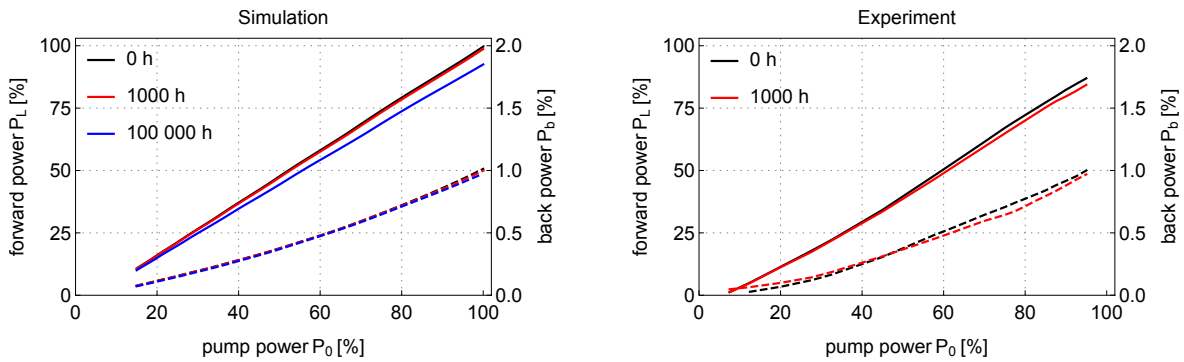

Figure 5: Simulated (left) and experimental (right) power curves for an industrial standard fiber. Solid / left axis: forward power (LP_{01}), dashed / right axis: back power (core and cladding). Black: $t = 0$ h, red: $t = 1000$ h, blue: $t = 100\,000$ h.

fibers with a comparatively high heat load. In contrast, Figure 5 shows the results for a setup using a fiber according to the current industrial standard (with a lower heat load). In this case, the simulation does not exhibit any sign of TMI anymore, even for simulated test durations of 100 000 h. Over this long time, only a slight degradation ($\approx 5\%$) of the laser power is observed due to additional PD induced absorption. As there is no corresponding increase of the back power (i. e. cladding light), this effect is not caused by TMI, but solely by direct absorption. On the contrary, the back power is slightly reduced due to absorption as well.

The corresponding experiment has not yet completed 100 000 h in the laboratory, but in the first 1 000 hours of operation, no noticeable degradation is observed, which agrees very well with the predicted behaviour.

Conclusion

We presented a hierarchical numerical approach that allows to first precalculate the transverse spatiotemporal distribution of the photodarkening losses over typical lifetimes of fiber lasers, and then apply the precalculated data to a scalar coupled-mode model of the full length fiber laser cavity. The effects of mode competition, laser gain, mode energy transfer and bend losses are considered in this model, as well as the measured refractive index distribution and doping profile of the actual fiber.

As a result, it is possible to perform virtual long term tests simulating several 10 000 hours of laser operation in a few hours. The numerical results agree well with experimental evidence. The transverse distribution of photodarkening losses in the fiber and the mode coupling gain can be analysed at any cross section along the fiber length, which enables the development of advanced mitigation strategies.

References

1. A. V. Smith and J. J. Smith, Mode instability in high power fiber amplifiers, *Opt. Express* **19**(11), 10180–10192 (2011)

2. H.-J. Otto *et al.*, Impact of photodarkening on the mode instability threshold, *Opt. Express* **23**(12), 15265–15277 (2015)

3. B. G. Ward, Modeling of transient modal instability in fiber amplifiers, *Opt. Express* **21**(10), 12053–12067 (2013)

4. K. R. Hansen *et al.*, Thermally induced mode coupling in rare-earth doped fiber amplifiers, *Opt. Lett.* **37**(12), 2382–2384 (2012)

5. L. Dong, Stimulated thermal Rayleigh scattering in optical fibers, *Opt. Express* **21**(3), 2642–2656 (2013)

6. C. Jauregui *et al.*, Temperature-induced index gratings and their impact on mode instabilities in high-power fiber laser systems, *Opt. Express* **20**(1), 440–451 (2012)

7. O. Antipov *et al.*, Influence of a backward reflection on low-threshold mode instability in Yb^{3+}-doped few-mode fiber amplifiers, *Opt. Express* **24**(13), 14871–14879 (2016)

8. C. Jauregui *et al.*, Simplified modelling the mode instability threshold of high power fiber amplifiers in the presence of photodarkening, *Opt. Express* **23**(16), 20203–20218 (2015)

9. J. J. Koponen *et al.*, Measuring photodarkening from single-mode ytterbium doped silica fibers, *Opt. Express* **14**(24), 11539–11544 (2006)